# Thermal Insights and Predictive Modeling of Axial Piston Pumps: A Journey to a High-Fidelity Digital Twin

**Roman Ivantysyn and Jürgen Weber**

*Institute of Mechatronic Engineering, Technische Universität Dresden,*
*Helmholtzstrasse 7a, 01069 Dresden,*
*E-mail: roman.ivantysyn@tu-dresden.de, fluidtronik@mailbox.tu-dresden.de*

## Abstract.

This paper presents a novel investigation into the modeling of axial piston pumps, with a focus on identifying the essential and non-essential measures for achieving high accuracy in thermal and efficiency prediction. A notable highlight is the first-ever published dataset of simultaneous high-dynamic temperature and pressure measurements within the displacement chamber of an operating pump, accompanied by detailed monitoring of its thermal behavior. This unique experimental foundation provides unprecedented insight into the impact of various modeling assumptions on the predictive accuracy of digital twins.

Highlighting the critical balance between model complexity and computational efficiency, the study identifies which assumptions can be safely made without compromising model fidelity and which require more careful consideration. Through careful analysis, it demonstrates how specific measures, such as accounting for component wear, manufacturing tolerances, and incorporating real-world temperature variations, significantly improve the accuracy of the model.

This work not only advances theoretical understanding, but also sets new benchmarks for practical modeling strategies, paving the way for advances in hydraulic system optimization and predictive maintenance offering a physic-based model rather than complex black box models. The insights gained from this study underscore the importance of a nuanced approach to model development and mark a new phase in the precision engineering of axial piston pumps.

**Keywords**. Digital Twin, Thermal Modeling, Tribology, Efficiency, Thermal Boundary Conditions, High-Dynamic Temperature Measurements

## 1. INTRODUCTION

The hydraulic industry exhibits remarkable versatility, with positive displacement units gaining prominence due to their superior power density, efficiency, and durability. These attributes render them indispensable in a wide range of demanding environments, from space aviation to various mobile applications, continuous industrial manufacturing processes, and specialized domains like subsea robotics. A common thread among these applications is the

uncompromising need to avoid failure, coupled with an increasing emphasis on enhancing efficiency in response to escalating energy costs and the imperative to reduce emissions. Mobile machinery, which represents the largest market segment for hydraulic components, is undergoing a transformative shift towards sustainability, spurred by the electrification movement. In this new era, hydraulic pumps will be integrated within interconnected components, necessitating advanced feedback mechanisms for real-time efficiency monitoring and performance prediction across diverse operational conditions.

The advent of high-fidelity digital twins promises to revolutionize this landscape, offering a virtual repository for machine operators, controllers, and system optimization algorithms. The rise of powerful numerical tools now allows for a cost-effective creation of digital twins within a simulation environment, avoiding the need to acquire expensive test-rig experiments and difficult to gather field data sets for machine learning algorithms.

This paper will demonstrate how a digital twin framework can be build using Caspar FSTI and outlines the essential steps to ensure a precise alignment between empirical measurements and simulation outcomes.

## 2. PRIOR WORK AND RESEARCH GOAL

The primary objective of the presented research is to demonstrate the feasibility of building a digital twin for hydraulic components, specifically axial piston pumps, leveraging a physics-based numerical model. This approach prioritizes a physics-driven framework over traditional black box models, offering scalable predictability across an expansive spectrum of components without necessitating extensive data collection. The challenge of amassing sufficient training data to encompass all operational scenarios of piston pumps is particularly acute for smaller hydraulic suppliers. Therefore, a cycle and system independent approach is required to allow scaling between various sizes and manufactures all within a virtual environment.

Previous studies have underscored the potential of machine learning-based black box models, with several achieving noteworthy outcomes, some of which are currently in practical use [1], [2], [3]. However, these models are generally restricted to specific pump series and use cases, such as stationary hydraulics with repetitive cycles, heavily reliant on high-frequency data from sophisticated sensors, electronics, and rapid communication technologies. Minor alterations, like relocating a sensor or changing the system’s impedance, can significantly impact the systems' response characteristics, complicating the scalability of these solutions across a wide range of applications. An additional hurdle for the black-box models entails the requisite collaboration between machine Original Equipment Manufacturers (OEMs), responsible for implementing and operating these models, and the pump manufacturers, who have the knowledge about their components but typically lack access to the machine's field data. Moreover, the inherent nonlinearity of lubricating gaps — which are critical for the system losses — remains elusive to even advanced physics-informed machine learning techniques.

The author has published previous work that validated the predictive capability of numerical pump models and demonstrated the potential of using cost-effective, reliable, and low-bandwidth temperature sensors to accurately predict pump efficiency and power losses. [4], [5], [6], [7]. By creating a high-fidelity numerical model, the bulk of computational demands

can be transferred to a controllable virtual environment, minimizing the reliance on physical data collection, which remains feasible with current technology and is system agnostic. The use of temperature as an efficiency predictor, although not novel as evidenced by the work of Schlösser and Renius, is innovatively applied here to transient data analysis rather than solely steady-state conditions — a crucial distinction given the impracticality of maintaining steady-state operations in mobile machinery, a limitation that has precluded the implementation of existing models in real-world settings [8], [9], [10].

This paper will present the general feasibility of a physics-based numerical twin for axial piston pumps based on the numerical tool Caspar FSTI for real world applications. By being able to accurately predict the gap heights in the lubricating gaps within a digital twin allows for the prediction of the entire pump's power losses, forecasting thermal variations in both components and fluid, and adjusting for performance shifts due to manufacturing tolerances. In detail this paper will:

- Present novel measurements in a rotating cylinder block, allowing for a deeper look inside the pump rotating kit.
- Demonstrate the conversion of transient data into comparable steady-state conditions with a steady-state numerical twin.
- Outline the necessary modelling depth of the twin to accurately predict real world applications.
- Emphasize the importance of incorporating wear modeling due to its significant impact on pump performance.
- Examine the effects of manufacturing tolerances on power losses and how the model can be used to predict these factors.

## 3. MEASUREMENTS

This chapter will showcase the measurement setup, highlight key measurements, and then present interesting trends and patterns that can be used to validate the simulation, enhance the virtual model and in general broaden the thermal understanding of axial piston pumps.

### *3.1. Measurement Set-Up*

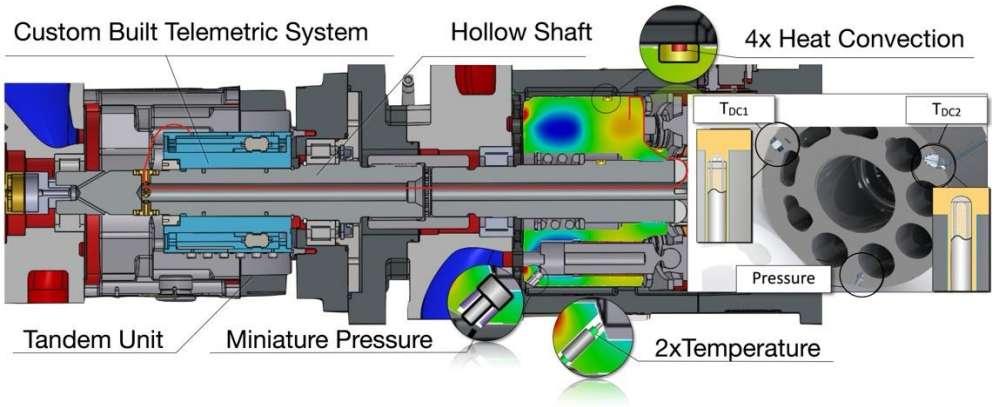


Figure 3.1. Measurement Set-up System Capturing 20x Temperature inside the Block, Pressure and Temperature in the Piston Chamber and Heat Transfer on the Surface.

A 160 cc open-circuit axial piston pump of the swash plate type was used as the test specimen for the temperature evaluation of the cylinder block. Prior publications have shown that measuring the cylinder blocks temperature is especially suitable for the efficiency evaluation of the entire pump, as it is the central element of the rotating kit and is affected by all lubricating gaps of the pump [4]. The utilized set-up is shown in Figure 3.1. An array of sensors was installed, including 20 temperature sensors capturing the cylinder block's temperature field, 4 heat-convection coefficients on the surface of the block (outside wall, shaft- and neck-surface) and high-speed pressure and temperature sensors monitoring the pressure build-up and corresponding transient temperature response of the compressed fluid. The locations of the thermocouples are illustrated in Figure 4.4. The data were transferred with an in-house built telemetric system that allowed for both the larger number of sensors and the fluent switch between high and low frequency data acquisition.
The heat convection coefficient sensors (h-sensors) capture the heat loss on the surface by heating a small resistance that also serves as a temperature sensor. The functionality was described in previous publications by Uffrecht et. al. [4], [11], [12], [13], [14]. The heat transfer was never measured in a working pump environment, allowing to validate CFD models in hydraulic fluid applications for the first time. A comprehensive comparison of different CFD-modeling techniques using various software approaches and comparing them to the measured trends will be published simultaneously to this paper in a different conference [15]. Figure 3.2 presents the measured trends for various surfaces with speed and change in displacement. The cylinder block (CB) outside wall surface only changes its heat exchange rate with speed and is independent of pressure and swash plate angle. The top region of the block however shows an increasing heat exchange rate with lower angles. Regions of high turbulences such as the piston or slipper can exceed the cylinder blocks convection rate due to local eddies increasing the boundary layer flow speed even though they have smaller angular velocities.

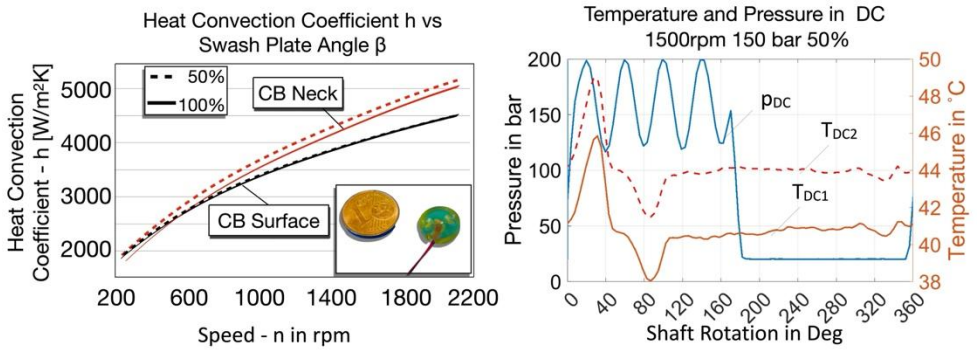


Figure 3.2. Sample Measurement of the Heat Convection and Pressure and Temperature inside the Displacement Chamber (DC)

By developing both the sensor and telemetry systems, as well as DAQ systems, in-house, it is possible to achieve high accuracy with maximum flexibility. This was demonstrated by capturing high-speed measurements simultaneous to the low-frequency temperature and h-sensors. By combining numerical gap results with FEM-Analysis it was possible to accurately predict the precise loading on the cylinder block and forecast the durability of the cylinder block for high pressure usage for each design option. The chosen design was designed to withstand at least 60 hours of testing at 300 bar. The resulting sensor

arrangement allowed the installation of two high-speed thermocouples and a high-speed miniature pressure sensor all within a cylinder block that featured over 30 other sensors, as some of the 20 temperature locations were installed redundantly. Two types of temperature sensors were used. The first sensor type (labeled '$T_{DC1}$' in Figure 3.1) features an open tip, exposing the 0.1mm wire used to measure the temperature. This allowed for minimal heat capacity and enabling the capture of temperature changes in the nanosecond regime. Naturally, the tip is very fragile and cannot be placed inside the flow path. The second thermocouple, '$T_{DC2}$', features the same small wire thickness as $T_{DC1}$ but has a small protective cap. This added robustness allowed to protrude the sensor further into the flow, to capture different boundary layers. However, after inspecting the pump post-measurement, it was revealed that this second sensor was touching the wall, essentially measuring the wall temperature from the inside. Initially it was feared that the added robustness slightly increasing its heat capacity decreasing its reaction time slightly. However, the measurement results are conclusive that in this application, pump speeds up to 2100 rpm and pressure build-up rates of 150 bar/ms, both sensors yielded fast enough response rates to follow the pressurization inside the displacement chamber as can be seen for 1500 rpm and 150 bar in Figure 3.2. The measurement concluded shortly before this paper was written; therefore, a fundamental analysis will be published in the future.

However, several very interesting observations can be made at the current analysis stage. The temperature response of the fluid shows a small lag for both sensors of 1ms at high speed, by peaking later than the fluid pressure. However, the sensors are fast enough, as the reaction to pressure is immediate even at 2100 rpm. This lag seems to be independent of speed, indicating a geometrical cause. During the change from high to low pressure the fluid is confined for a short instance to one piston bore, before opening to the high-pressure (HP)-kidney of valve plate. During this time the temperature spikes considerably, but never peaks at the same time as the pressure, rather it continues to rise until the pistons opens to the HP-port. This indicates that the fluid temperature rise with pressure is not instantaneous. After re-connecting with the other HP-pistons through the HP-kidney the temperature in the fluid drops significantly, signally a thermodynamic loss. Surprisingly this temperature drop even falls below the suction stroke (180˚ - 360˚) temperature, in certain condition even below the 35˚C port temperature. This phenomenon occurs both in transient and steady state at all pressure and speed levels and is captured by both sensors ruling out a faulty sensor. This means that even during steady state operation the piston pressurization cannot be simplified as an adiabatic process. Another interesting finding is that while the temperature response to the pressurization is clearly visible and lies within 2-8K for pressures of 50-250 bar, there is no temperature change in the displacement chamber during the suction stroke. While all measurements were performed at 35˚C inlet temperature (measured directly at the inlet), the temperature in the displacement chamber was always several degrees above this value. One must assume that the turbulent flow through the suction port quickly heats the fluid by several degrees. This temperature increase as a function of speed is depicted in the blue curve in Figure 3.3.

The cylinder block temperature was captured both in transient and steady state conditions, where steady state was defined as <0.1K/min change in all installed sensors relative to the inlet temperature. This thermal equilibrium condition was typically reached in 10-15 min for small changes in the operating point or 15-30 min for larger speed or pressure changes. By analyzing the steady state temperature and efficiency one can gain a fundamental

understanding of the lubricating gaps, as all other transient effects can mostly be neglected, although the temperature dip inside the displacement chamber clearly suggests limits to these assumptions.

To illustrate how the cylinder block temperature level changes with speed for a given pressure level, the min. max, and mean block temperatures are shown in Figure 3.3 across the pumps' speed range for 100 bar. The total measured pump efficiency is shown in grey, while the measured fluid temperature in the suction stroke of the displacement chamber ($T_{DC}$) is depicted in blue and cyan. Both mean and maximum temperature rise significantly with speed, whereas the minimal temperature increases only slightly. The minimal block temperature is measured always near the displacement chamber (see Figure 4.5 and the cutout depicted). The minimum block temperature correlates exactly with the measured fluid temperature $T_{DC1}$ (blue circles) indicating a rather large heat transfer rate in the displacement chamber. The second temperature sensor in the displacement chamber ($T_{DC2}$ – shown in cyan color) turned out to touch the inside wall of the chamber. Hence it represents the temperature of the inside surface of the bore near the bottom of the displacement chamber, which shows a different trend with speed. It should be noted that the solid body temperature of the block is much higher in the area where the fluid temperature sensors were installed (bottom corner of the displacement chamber) as compared to further up towards the center of the middle of the chamber, where the minimal block temperature was captured. The shown graphic illustrates the temperature distribution at 1000 rpm and 100 bar around the displacement chamber. All measurements were standardized to 35˚C ±1˚C inlet temperature to guarantee uniformity across different operating conditions. Notably, the fluid temperature inside the displacement chamber never reaches this 35˚, indicating a high heat transfer rate in the suction port, increasing the fluid temperature notably. At 100 bar, the minimal block temperature decreases with speed, indicating that despite the block temperature increasing, the fluid temperature decreases. This is because the higher flow rate at increased speeds (with the fluid passing through the inlet port in roughly 15 ms at 2100 rpm) reduces the time the fluid remains in the pump. Consequently, the fluid has less time to absorb heat, resulting in a lower fluid temperature.

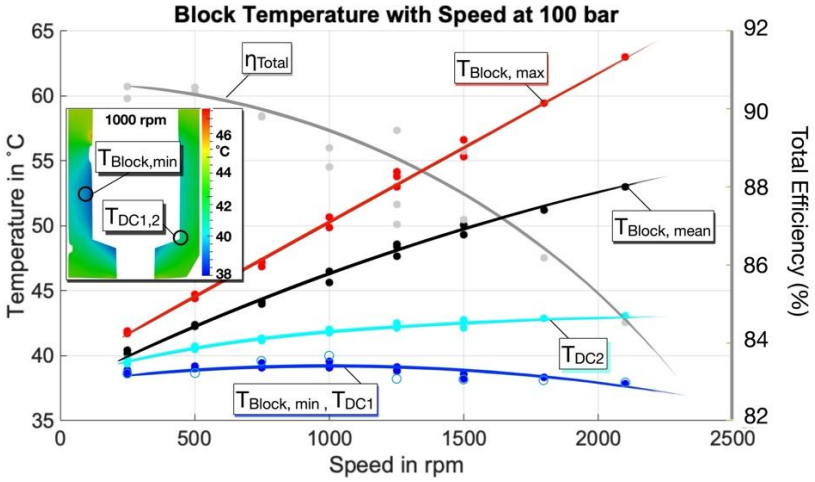


Figure 3.3. Measured Temperature and Efficiency Trend with Speed at 35˚C Inlet, 100 bar and Full Displacement.

The temperature increase in this pump is mainly due to speed and less affected by pressure, as can be seen in Figure 3.4. Shown on the left is the maximum measured cylinder block temperature with speed and pressure at 100% swash plate angle. The hydraulic power output is shown in the black contour lines. Shown are also the total and partial efficiencies for reference. While the temperature field is influenced by both viscous and volumetric losses occurring in the lubricating gaps, no discernible pattern emerges that aligns consistently with power output and efficiency lines. This suggests that, although temperature rise correlates with power output and losses, it intersects with both power and efficiency metrics in a manner that prevents a straightforward trend from being established. The method for leveraging this metric to accurately gauge efficiencies will be elaborated in the following section by means of simulation models that can link gap losses with efficiency and temperature.

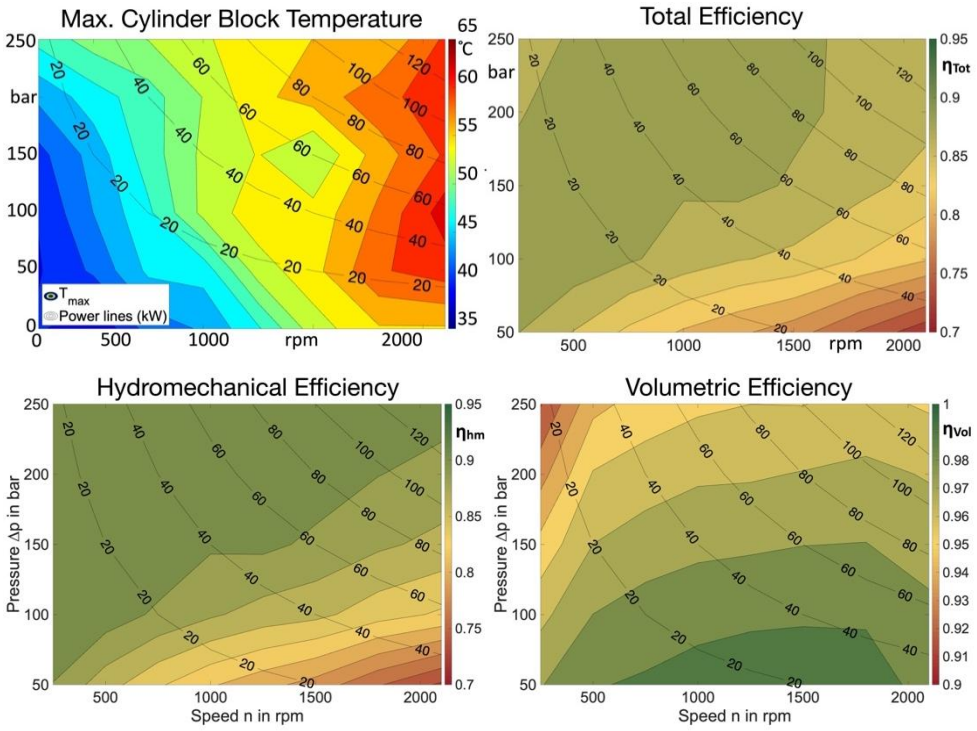


Figure 3.4. Captured Cylinder Block Temperature and Efficiency Field of an 160cc Axial Piston Pump at Full Displacement.

## 4. DIGITAL TWIN OF THE ROTATING KIT OF AN AXIAL PISTON PUMP

The numerical model used for predicting the power losses occurring in the lubricating gaps is called Caspar FSTI. The model was developed by Monika Ivantysynova and her team of researchers over a 30-year time span and several fluid power centers. It was specifically developed for piston pumps, enabling efficient modeling without the need for in-depth knowledge of numerical techniques and mesh studies. It captures the necessary micromotion and part deformation both due to pressure and temperature, which was shown to have a tremendous effect on the performance on the tribological interfaces [16]. The tool was

validated for each lubricating gap using both temperature and gap height measurements [4], [5], [17], [18], [19], [20], [21], [22]. While simulating just one gap interface is common practice and practical for relative improvement studies all three gaps need to be modelled to capture the entire pump efficiency and thermal behavior as the gaps affect each other.

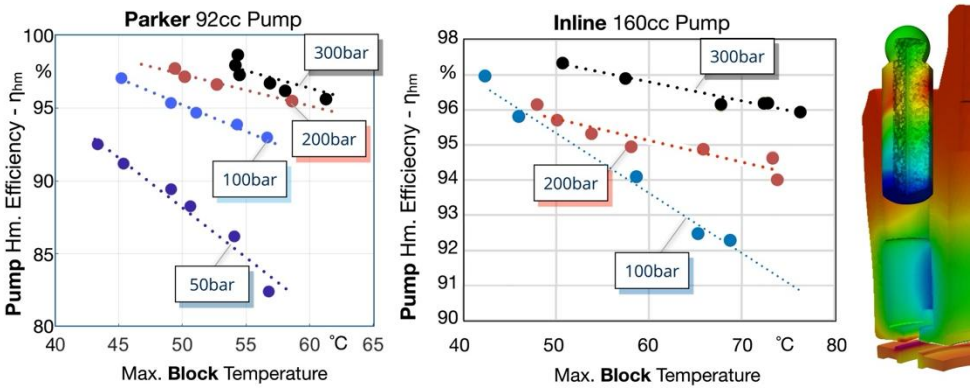


Figure 4.1 Digital Twin Predicts Pump Efficiency and Cylinder Block Temperature Correlation for Two Different Pumps.

Such a complete model was built for two different high-pressure axial piston pumps. A 92cc pump from Parker Hannifin and a 160cc pump from Inline Hydraulics were analyzed. Both pumps feature no special components such as inverse pistons, spherical valve plates or bushing less pistons and can therefore be taken as a good representation of the average piston pump on the market.

Both models predict a linear correlation between the hydromechanical efficiency of the entire pump and the max. cylinder block surface temperature. Shown in Figure 4.1 is the simulated trend for both pumps. As can be seen, there is a direct correlation between efficiency and temperature at each pressure. A similar trend can be made for the volumetric and total efficiency as was shown in [4]. In the same publication the trend was validated with steady state measurements, confirming that measuring the surface temperature of the cylinder block allows for a direct correlation with the total and partial efficiencies of the entire pump. A similar trend can also be made with the steady state leakage and housing temperature, as they follow the maximum block temperature quite well. However, for real world applications it is not feasible to wait for steady state. The cylinder block reacts instantly to any operational change, allowing for a transient model.

### *4.1. Efficiency Prediction using Transient Temperatures*

A typical transient condition change is shown in Figure 4.2. The pump goes through a 250 rpm speed change in a 10 s time frame. While this change is not particularly dynamic, it greatly captures the temperature lag of the fluid and housing temperatures in comparison to the cylinder block. As can be seen in the thicker blue curve, the cylinder block reacts instantly and without any noticeable lag to the speed change, increasing its temperature by more than 2K in the 10 s time frame it took to change the speed. While it has not reached steady state, it exhibits an easily detectible temperature increase. Meanwhile, the fluid temperatures (inlet, outlet and leakage) change minuscule in this 60s time frame, not reliably

detectable for most temperature sensors. The housing temperature also does not change as it is reliant on the leakage temperature to conduct the heat generated in the rotating kit.

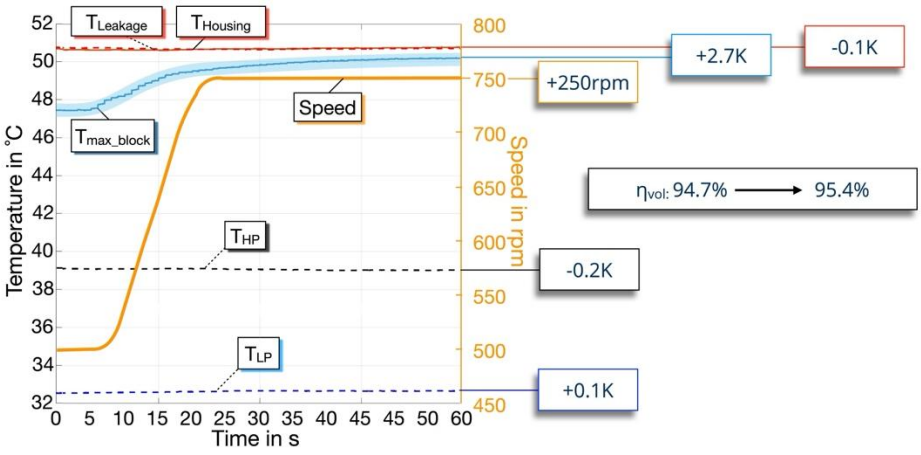


Figure 4.2 Fast Transient Response of the Cylinder Block in Comparison to the Fluid and Housing Temperatures.

While the speed change was small it caused a noticeable increase in volumetric efficiency, showcasing that the transient temperature is indeed capable of predicting transient efficiency changes. The volumetric efficiency $\eta_{vol}$ exhibits an inverse trend with block temperature as compared to the hydromechanical efficiency $\eta_{hm}$. Higher viscous losses increase heat losses which increase local component temperatures, causing a positive correlation between $\eta_{hm}$ and $T_{max,block}$. Higher volumetric efficiency means lower gap leakage, which causes less heat to be dissipated from the gap to the environment, causing an overall increase in component temperature. To be able to distinguish temperature increase due to higher friction or lower leakage, it is instrumental to predict the effect of gap height movement on distinct component temperature changes at various positions, e.g. where the hottest temperature occurs. In practice this means that at least 2-3 temperature locations need to be monitored on the cylinder block surface.

A digital twin allows for such a prediction, being trained on the physical behavior inside the lubricating gap, it can interpret each temperature change and predict even which component is causing the losses at this instance of time. As Caspar FSTI requires thermal equilibrium to keep simulation time reasonable, it is necessary to convert the transient temperature change to a steady state value, which can in turn be used with the digital twin.

Such transient model was developed using over 200 transient temperature rises/and falls with their corresponding measured steady state values. Such a rise is shown Figure 4.3 for the same 250 rpm increase as shown earlier. Left in the figure is the full 35 min of data, shown for one of the sensors inside the cylinder block. Steady state ($\Delta T/\Delta t$ <=0.1K/min) was reached for this operating condition after 30 min at 51.1˚C. The transient predictive model was fed with just 30 seconds of this data and predicts a steady state temperature of 51.2˚C after 25 min.

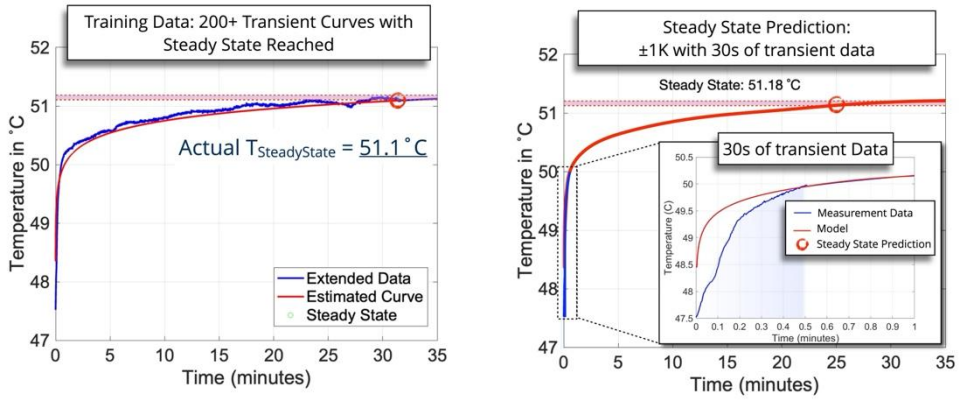


Figure 4.3. Prediction Model to Convert Transient Data to Steady State Data.

This model also works for temperature drops and can predict thermal steady state conditions with a ±0.1K accuracy, which was determined to be accurate enough as most efficiency changes cause temperature increase of more than 1K, as was demonstrated in Figure 4.2 for a less than 1% change in volumetric efficiency.

As was established in the previous section, it is quite feasible to monitor the current pump efficiency using the surface temperature of the cylinder block. There are multiple methods to capturing this temperature, whether through conduction (via a spring-loaded sensor), radiation (using an optical method) or by wireless transmission using an sender/receiver principle. The possibilities are endless and certainly do not require a complicated set up as was done for this research endeavor. The number of measurement locations could vary for each pump, but for the studied pumps two locations are sufficient to capture the maximum temperature. One sensor at the bottom near the valve plate and one towards the top on the cylinder block outside surface will suffice. While it is certainly possible to substitute some rotating sensors with non-moving stationary sensors such as on the valve plate, it will certainly require more sensors stationary sensors as compared to rotating ones. This is because the hot spots move on the valve plate between operating conditions as was shown in [5], [7], [22]. As the sensors-problem can certainly be solved with good engineering work, the question arises what model depth is necessary to build an accurate digital twin using Caspar FSTI or similar numerical models.

### *4.2. Required Model Accuracy and Boundary Conditions*

As in every simulation model certain assumptions must be made to simplify reality. Caspar FSTI certainly is no exception and requires for example steady-state operating conditions and corresponding thermal boundary conditions including the port temperatures. In addition, the gap geometry needs to be defined using geometrical parameters such as diameters and notches. These components deviate within the manufacturing tolerance band in both shape and surface topology. Choosing the right dimension and determining which parameters are more important than others, requires experience. This paper is meant to give some helpful guidance in this process. To capture the deformation due to pressure loading or temperature expansion a mesh needs to be generated for each gap defining surface. As is typical for any FEM-Model, these meshes require geometrical simplifications and boundary conditions.

This section will show how the digital twin of the 160cc Inline pump was developed over time and what effect the model improvements had on the efficiency and temperature prediction. A mid speed and mid pressure operating condition will be used to showcase the changes throughout time, as extreme conditions can cause the model to numerically diverge due to mixed friction. The run-in process is period in the first couple of hours of the pump, where most pumps go through an abrasion process, which can vary from pump to pump in intensity. This run-process needs to be captured either by simulation prediction or by measuring part dimensions to capture the true efficiency and temperature.

Figure 4.4 shows the initial simulation result in terms of cylinder block temperature with speed for 100 bar and 100% displacement. In comparison is the measured temperature distribution. Shown are in red the maximum and in black the average block temperature. The simulation is in dashed and the measurement in full lines. The simulation shows a general good fit, especially at low speeds, however at high speeds the maximum temperature deviates significantly when comparing the simulation to measurement. For these first simulations there were no pump measurements available. Hence the boundary conditions were based on initial assumptions and experience. Other simplifications were no pressure and temperature deformation at the bushing, as there was an error in the part meshes, which had to be redone. All dimensions were based on CAD-information and all surfaces were flat, meaning no surface topology or edge rounding was applied.

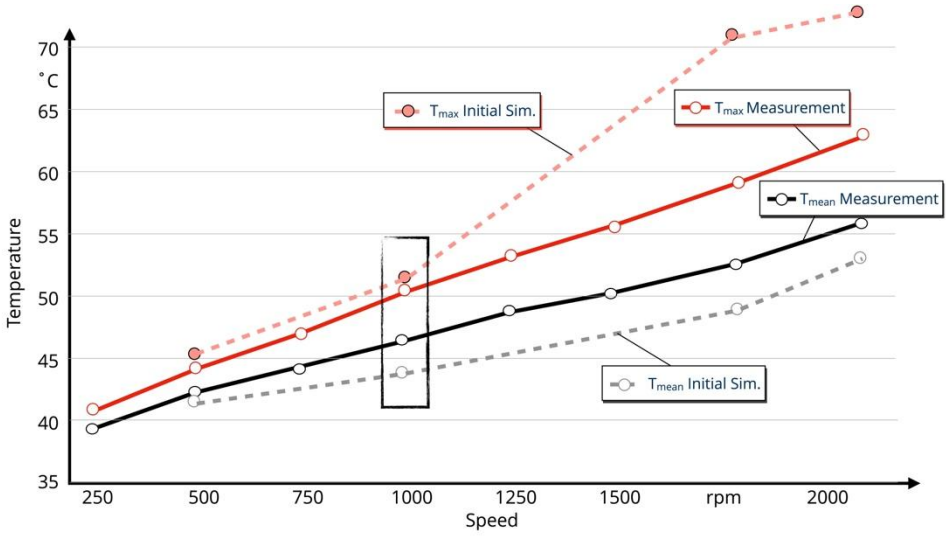


Figure 4.4. Initial Simulation Model Predicts Trend but does not Match Maximum Temperature at 100 bar and Full Displacement.

Despite these simplifications the initial simulation results were a good match between simulation and measurement in terms of overall temperature. 1000 rpm is highlighted as it will be discussed in more detail in the upcoming paragraphs. While the initial temperature level at this condition looks promising, a closer look shows significant deviations, exemplifying that not just one metric should be used to validate results.

Figure 4.5 shows the measured temperature field at the highlighted 1000 rpm 100 bar 100 % operating condition, along with the measured efficiency and steady state fluid temperatures. The colored dots on the left chart represent the 19 unique measurement locations, with one additional thermocouple being placed in the surrounding oil at the top of the block, to capture the leakage temperature near the block surface. On the right side is the initial simulated temperature field of the cylinder block and the predicted pump efficiency, based on the losses occurred in all three lubricating gaps. The overall temperature trend is similar, where the hottest temperatures occur on the valve plate gap, and the coldest around the displacement chamber. However, the temperature levels don't match. The upper half of the cylinder block is around 48˚C in measurement, where the simulation predicts no hot spots here with temperatures below 44˚C. False hot spots are being predicted by the simulation model at the bottom of the inner bushing. At this stage the simulation model did not account for bushing deformation, which caused contact and unrealistically high gap pressures and temperatures.

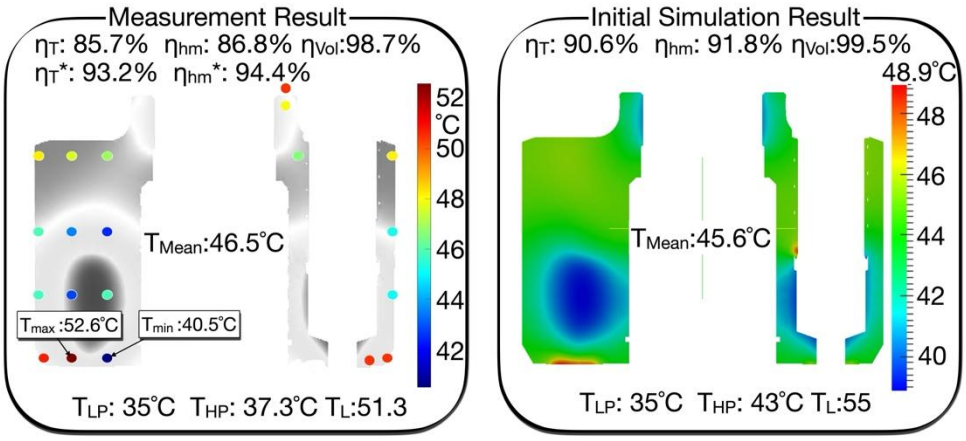


Figure 4.5. Measured (Left) Hot and Cold Spots are not Captured Accurately with Initial Simulation (Right) at 1000 rpm and 100 bar 100%.

For both the simulation and measurement the total and partial efficiencies are listed. For the measurement a second set of efficiencies is shown, marked with an asterisk(*). This adjusted efficiency is an estimated total and hydromechanical efficiency based on just the gap losses in the rotating kit, excluding the bearing and churning losses. This adjusted efficiency was estimated by subtracting the pump losses at the same speed at 0 bar, essentially subtracting estimated parasitic losses outside the rotating kit. This method cannot be applied at all operating conditions, as viscous friction also occurs without pressure especially at low or very high speed. However, at 1000 rpm 0 bar this pump exhibits nearly no tribological losses as confirmed by the simulation, measured block temperature and measured efficiency extrapolation (projecting $\eta_{hm}$ to the 0 bar intersect), allowing for such an estimation. This estimated gap efficiency serves as a target for the simulation, allowing for a direct comparison between measurement and simulation.

The initial simulation model, which lacks bushing deformation and component wear, overestimates the losses, when compared to $\eta_{total*}$, which are mainly due to higher torque losses. In conclusion, the initial simulation gives a relatively good thermal preview, but lacks

the detail to predict the losses and temperature hot spots correctly, mostly due to the missing thermal and pressure deformation in the piston/bushing sealing gap.

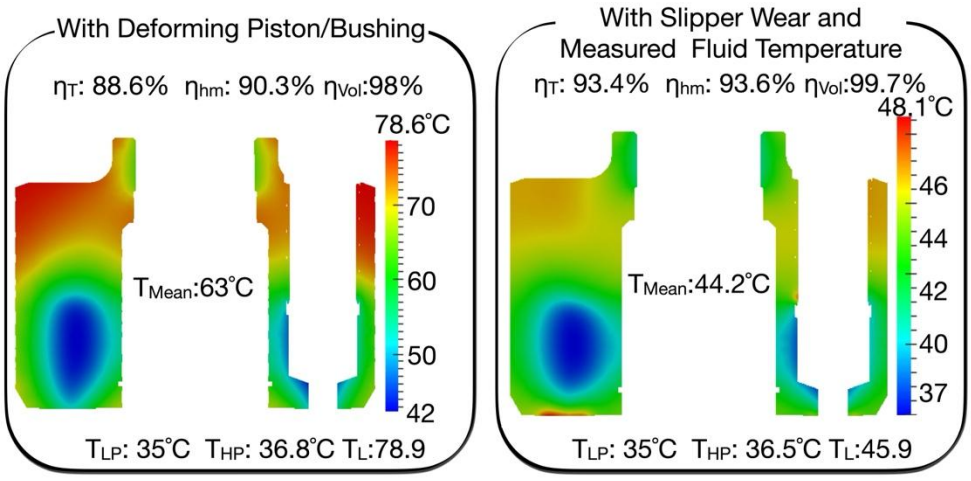


Figure 4.6. Influence of Increasing Modelling Complexity on the Predicted Temperature Field and the Efficiency at 1000 rpm 100 bar and 100%.

After including the elastic deformation of the bushing and piston, the overall temperature increased significantly mainly driven by the higher leakage temperature, as seen in Figure 4.6 on the left. While the efficiency now compares closer to the measured total efficiency, it lies well below the anticipated adjusted efficiencies, forecasting higher losses and higher temperatures. The hot spot locations however are now closer to the measurements, signaling that the gap behavior is now captured correctly just not at the correct power losses and thermal boundary conditions. The reason why the leakage temperature was much higher than the measurement can be explained by the fact that these simulations were performed before any pump measurements were recorded. Without any measurement data the inputs are reliant on an additional thermal model, which converts simulated gap losses to fluid temperatures [23]. As the losses were higher, the model predicted significantly increased leakage temperature levels. As this is an iterative process, the new boundary conditions are calculated after the simulation finished and then the simulation is restarted with the newly calculated temperatures. Several iterations are necessary to converge on a final solution. If the parts wear-in significantly this process can be quite lengthy without appropriate measurement data.

For the next simulation series (right temperature field in Figure 4.6), the first reference pump measurements were available. Thus, all simulation shown thus far relied on simulation models for their boundary inputs. As the reference pump was unmodified to ensure a reliable base, no cylinder block temperatures were available for validation or input. The measured fluid temperatures were now incorporated as the input for the simulation from here on out. Meanwhile it was discovered that the slipper performed poorly at several operating conditions, crashing with mixed friction and causing elevated friction losses. To improve this behavior, a wear model was used to predict the actual slipper surface geometry which was described in detail in [24], [25].

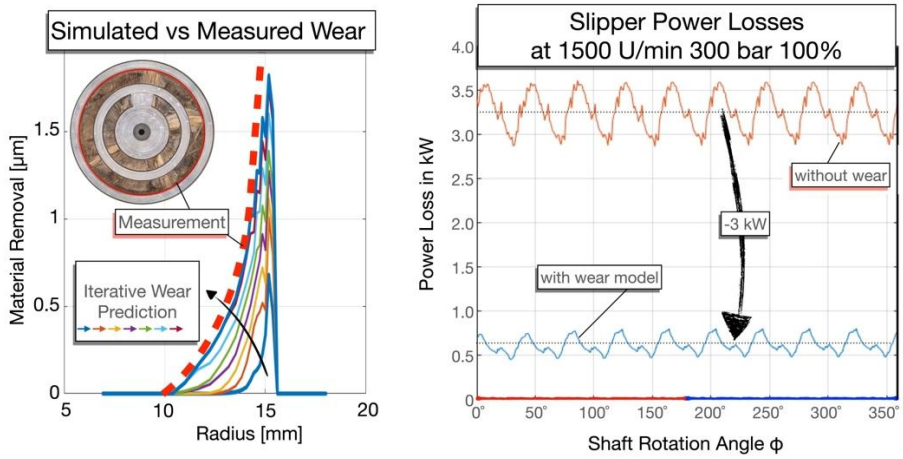


Figure 4.7. Slipper Edge Wear Decreases Power Losses Significantly.

The wear prediction is an iterative process, requiring a series of consecutive simulations slowly increasing wear with each step. The result of this pump was a 2 µm edge wear at the slipper sealing land. This edge wear seems rather miniscule, however the differences resulted in significant changes to the torque losses and power losses. As shown in Figure 4.7 on the right, the power losses decreased by over 3 kW for a high-speed high-pressure operating condition mostly due to a 50% reduction in viscous losses. The left graphic shows the predicted vs measured slipper sealing land geometry, as can be seen they match both in trend as well as in magnitude. However, as the iterative wear-in process is rather time consuming, it is recommended to measure these actual surface profiles if available. With measured fluid temperatures and the described slipper wear-in profile, the simulation results improved as shown on the right side of Figure 4.6. The simulation field now shows a better match with measurement, both showing the same trends and similar temperature magnitudes. With matching temperatures, the efficiencies also come closer to the measurement, both in hydromechanical and total efficiency. However, the leakage was underpredicted, which will be improved in the next section.

### *4.3. Correct Part Dimensions*

To this point all shown simulation results were based on nominal CAD dimensions. To improve the simulation further all gap defining parts were measured both with a Keyence 3D optical profilometer and a 1D stylus-profilometer. A sample results for the relevant piston dimensions are shown in Figure 4.8

Shown are the piston length, diameter, and surface topology, which were averaged across all 9 pistons. These measurements were performed for both new and worn parts, albeit not from the same charge. During these measurements it is important to understand the limits of lubricating gaps. For example, the sealing length of the piston is only relevant for the first 100 µm as shown in the top figure. As the piston has chamfers for easier assembly, it is important to correctly determine the actual sealing length as any overestimation would cause a change in hydrodynamic pressure built up. To further improve the simulation, it is also recommended to input the actual sealing surface topology, as it also influences the results, as shown in the slipper wear.

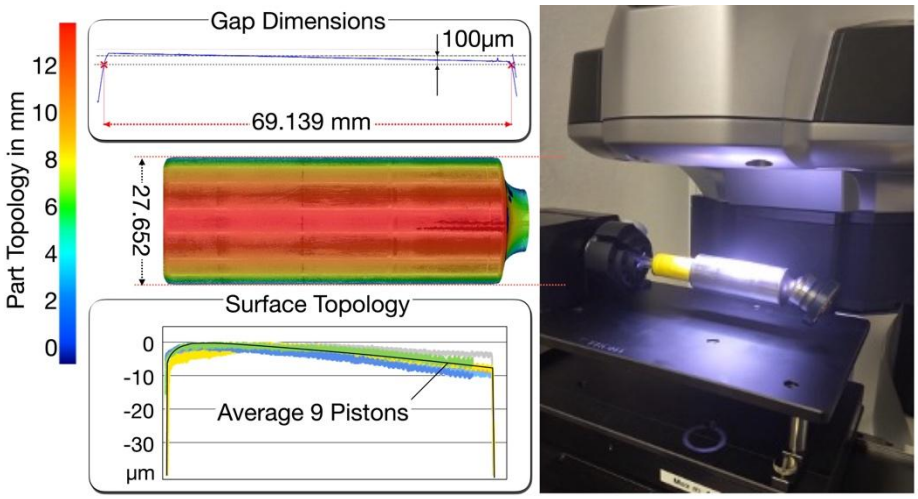


Figure 4.8. Actual Part Dimensions Measured with Profilometers

To demonstrate the effect miniscule dimensional changes, have on the efficiency and temperature, a dimensional case study was performed for the gap defining dimensions of the valve plate/cylinder block interface. Figure 4.9 shows the several simulation outputs for various dimensional inputs. The y-axis shows the power loss sum of 4 operating points, composed of two speed levels (500 rpm & 1800 rpm) and two pressures (100 bar and 300 bar) shown relative to the output power. The x-axis shows 5 different dimensional inputs: The minimum, maximum and nominal sealing land width, and the sealing land dimensions of a newly manufactured and a worn valve plate.

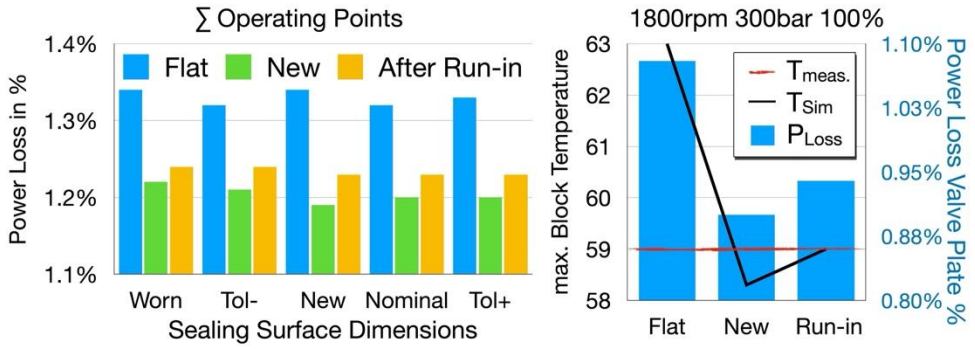


Figure 4.9. Change in Efficiency with Part Dimensions.

The different bar colors represent different surface definitions. The blue bar is a perfectly flat surface with sharp edges. The simulation results for the actual measured surface topology are represented by the green and orange bar for new and run-in respectively. There is a clear difference in power loss between the flat surface topology and the actual topologies. The magnitudes may not be significant, but a clear trend is shown: The actual geometry paired with the actual surface shape has the lowest power losses for this set of operating conditions. After run-in the power losses increase. The change between the different gap dimensions is not very large, the biggest influence on the power losses

simulation error is the false assumption that the surface is flat. While it shouldn't be assumed that the shown curves are true for every pump and every interface, they do illustrate the impact some simplifications have on the accuracy of the result.

As it is not possible to isolate power losses occurring in the valve plate/ cylinder block interface from the measured total pump losses, the validation will need to be made through the temperature level as thermocouples were placed near this gap. The right side of the graph shows the corresponding temperature changes in the cylinder block gap for the measured dimensions after wear-in for three different surface profiles (flat, newly manufactured and run-in). This is meant to demonstrate the impact of surface topology on maximum temperature prediction and how sensitive the temperature is to even the slightest efficiency changes. The bar height represents the power loss in % for the operating condition: 1800 rpm 300 bar 100% displacement angle. While the change in power loss seems insignificant, there is a clear impact on the maximum gap temperature. The actual gap temperature, measured 2 mm below the running surface, is shown in red for the given operating point. The black line represents the simulated temperature at the same location and depth. With the right surface dimensions (worn) but the wrong flat surface profile the powerloss is over-estimated and the temperature is off by several degrees. By providing the manufactured surface topology the temperature error decreased below 1K. Finally with the correct dimensions and the correct topology the temperature matches exactly, allowing for the assumption that the gap height and therefore power losses are simulated correctly.

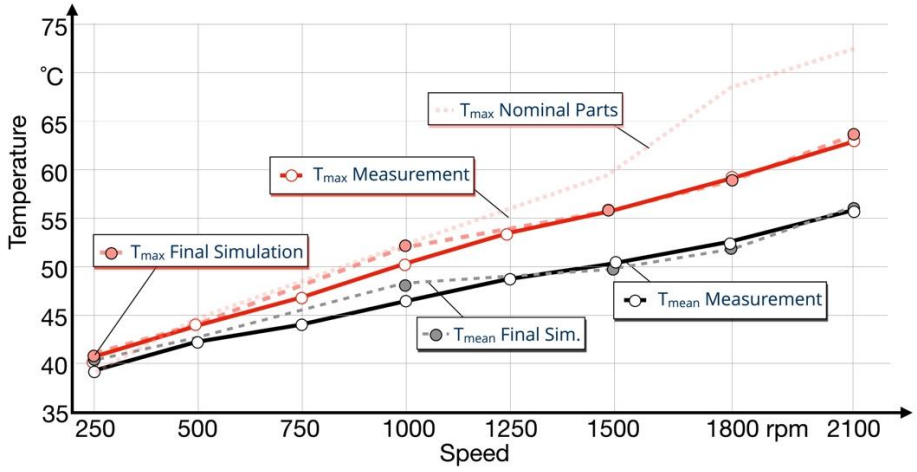


Figure 4.10. Final Output of the Digital Twin Compared to Measurement at Various Speeds at 100 bar and 100% Displacement Angle.

After improving the thermal boundary conditions by both incorporating the measured fluid temperatures and the measured heat convection coefficients, inputting the correct part dimensions and accounting for surface wear, the final simulated cylinder block temperatures can be seen in Figure 4.10 for various speeds as compared to measurement for 100 bar and 100% across the entire speed range of the pump. Now not only the temperature trends but also their magnitude match the measurement. This is true for both the average and the maximum temperature, with minor local differences. To demonstrate what impact the change to actual dimensions and measured surface topology has on the temperature, $T_{max}$ is

also shown for nominal valve plate parts with the same thermal boundary conditions (light red dashed line). The highest impact of these model improvements is observed at high speed. There are a still a few simplifications such as a perfectly flat piston and cylinder block surface, however as both temperature and efficiency match quite well, it can be assumed that these have a smaller impact on this pump.

## 5. CONCLUSION

This paper demonstrates the impact various modeling assumptions have on the accuracy of the simulated efficiency and temperature predictions for the entire rotating kit of an axial piston pump. It was shown that general trends are matched quite well when considering nominal CAD dimensions when part deformation is considered. Achieving precise temperature predictions necessitates integrating accurate port temperatures (inlet, outlet, leakage), ideally through measurement. For prototypes where no measurements are available, these temperatures can also be estimated with a thermal model that uses pump losses, if part wear is factored into the analysis. Predicting surface wear using Caspar FSTI is feasible, albeit through a time-intensive, iterative process evidently affected by temperature and contingent on assumed thermal boundary conditions. If available it is recommended to measure the surface run-in using precise profilometers, which yields more accurate results in less time. The incorporation of measurement results, particularly measuring part dimensions and surface topology before and after operational tests, is strongly advocated. This study underscores the profound impact of surface topology on simulation fidelity, with wear on the slipper and valve plate notably altering power losses and temperature dynamics. It was shown that for the valve plate the gap dimensions are less impactful than modeling the correct surface topology.

The high-frequency temperature measurements conducted in this study revealed critical insights into the thermal dynamics within the axial piston pump's displacement chamber. These measurements demonstrated that the fluid temperature response highly dynamic, changing withing milliseconds but lags slightly behind pressure changes, indicating a non-instantaneous heat transfer process. There are significant differences in the fluid temperature levels between the inlet port, the suction stroke, and the delivery stroke, as well as between the fluid and the wall temperature. Moreover, the observed temperature spikes during the transition from low to high pressure, followed by significant temperature drops, highlight the complexity of the thermodynamic interactions within the pump. A key finding is that adiabatic assumptions for the rapid pressurization in the pump is false, as even in this short amount of time temperature is transferred to the environment, resulting in an energetic loss that cools the fluid.

Furthermore, the findings highlight the degree of simulation detail achievable with Caspar FSTI, distinguishing between assumptions that exert minimal impact and those that significantly influence the outcomes. The digital twin developed for this study successfully forecasts efficiencies and temperatures across a range of nominal part dimensions and the full spectrum of manufacturing tolerances. This capability underscores the model's robustness in accurately predicting pump performance under various manufacturing variations, highlighting its practical utility in engineering applications.

## 6. REFERENCES


[1] M. Oppermann, "An investigation into failure prediction for mobile hydraulic systems," TUHH, Hamburg, Hamburg, 2007.

[2] T. Torikka, "Bewertung von Analyseverfahren zur Zustandsüberwachung einer Axialkolbenpumpe," 2010.

[3] A. Emad, "Self-Learning Condition Monitoring for Smart Electrohydraulic Drives," 2019.

[4] R. Ivantysyn, J. Weber, A. Kunze, and W. Uffrecht, "Thermal Analysis of the Cylinder Block of an Axial Piston Pump – The Key to Monitoring Efficiency," in *IFK2024*, 2024, pp. 1–21.

[5] R. Ivantysyn and J. Weber, "Investigation of the Thermal Behaviour in the Lubricating Gap of an Axial Piston Pump with Respect to Lifetime," in *11. IFK 2018*, 2018.

[6] R. Ivantysyn, A. Shorbagy, and J. Weber, "An Approach to Visualize Lifetime Limiting Factors in the Cylinder block / Valve Plate Gap in Axial Piston Pumps," in *FPMC2017-4327*, 2017, pp. 1–12.

[7] A. Shorbagy, R. Ivantysyn, F. Berthold, and J. Weber, "Holistic analysis of the tribological interfaces of an axial piston pump - Focusing on pump' s efficiency," in *IFK2022*, Aachen, 2022.

[8] W. M. J. Schlösser and K. Witt, "Thermodynamisches Messen in der Ölhydraulik." VDMA, 1976.

[9] J. Schlösser, "Thermodynamisches Messen des Gesamtwirkungsgrades and hydrostatischen Antrieben," *O + P: Zeitschrift für Fluidtechnik*, pp. 285–287, 1973.

[10] H. J. Matthies and K. T. Renius, *Einführung in die Ölhydraulik*. 2014. doi: 10.1007/978-3-658-06715-1.

[11] W. Uffrecht and A. Günther, "Electro-thermal measurment of heat transfer coefficients," in *ASME Turbo Expo 2012*, 2012.

[12] W. Uffrecht, A. Günther, and V. Caspary, "Kleine Thermistoren zur Messung von Wärmeübergangskoeffizienten," *Technisches Messen*, vol. 79, no. 12, pp. 549–558, 2012, doi: 10.1524/teme.2012.0230.

[13] G. Eschmann, A. Kuntze, W. Uffrecht, and S. Odenbach, "Measurement if heat transfer coefficients un gaseous flow - first test of a recent sensor concept for stationary and oscillating flow," in *ASME Turbo Expo 2014*, 2014, pp. 1–11.

[14] W. Uffrecht, B. Heinschke, A. Günther, V. Caspary, and S. Odenbach, "Measurement of heat transfer coefficients at up to 25,500g - A sensor test at a rotating free disk with complex telemetric instrumentation," *International Journal of Thermal Sciences*, vol. 96, pp. 331–344, 2015, doi: 10.1016/j.ijthermalsci.2015.03.006.

[15] R. Ivantysyn, A. Shorbagy, A. Vedpathak, and J. Weber, "Investigation of the Heat Conduction in Axial Piston Pumps by Measurement and Simulation," in *IEE GFPS 2024*, Hurtigsval, Sweden, 2024.

[16] S. Horn, R. Ivantysyn, and T. Schmidt, "Tribological properties of different slipper designs of an axial piston pump," in *IFK2024*, 2024, pp. 1–18.

[17] U. Wieczorek and M. Ivantysynova, "Computer aided optimization of bearing and sealing gaps in hydrostatic machines—the simulation tool Caspar," *International Journal of Fluid Power*, vol. 3, no. 1, pp. 7–20, 2002, doi: 10.1080/14399776.2002.10781124.

[18] A. Schenk, "Predicting Lubrication Performance Between the Slipper and Swashplate in Axial Piston Hydraulic Machines," Purdue University, 2014.

[19] M. Pelosi, "An Investigation on the Fluid-Structure Interaction of Piston/Cylinder Interface," Purdue University, 2012.

[20] M. Zecchi, "A novel fluid structure interaction and thermal model to predict the cylinder block/valve plate interface performance in swash plate type axial piston machines," Purdue University, West Lafayette, IN, 2013.

[21] S. Horn, R. Ivantysyn, and J. Weber, "Validated efficiency improvements by implementation of structures on the slipper surface of an axial piston pump," in *IEEE GFPS 2022*, Naples, 2022.

[22] R. Ivantysyn and J. Weber, "'Transparent Pump' – An approach to visualize lifetime limiting factors in axial piston pumps," in *ASME 2016 9th FPNI Ph.D Symposium on Fluid Power*, Florianapolis, Brazil, 2016.

[23] L. Shang and M. Ivantysynova, "Port and case flow temperature prediction for axial piston machines," *International Journal of Fluid Power*, vol. 16, no. 1, pp. 35–51, 2015, doi: 10.1080/14399776.2015.1016839.

[24] R. Ivantysyn, A. Shorbagy, and J. Weber, "Investigation of the Wear Behavior of the Slipper in an Axial Piston Pump by Means of Simulation and Measurement," in *12. IFK 2020*, 2020.

[25] R. Ivantysyn, A. Shorbagy, and P. J. Weber, "Analysis of the Run-in Behavior of Axial Piston Pumps," in *IEEE GFPS 2018*, Samara, Russia, 2018.